JPE 18-6-9

https://doi.org/10.6113/JPE.2018.18.6.1697
ISSN(Print): 1598-2092 / ISSN(Online): 2093-4718

Two Low-Loss Large Current Rectifiers Based on Low KVA Rating Wye-Connected Autotransformers

Fangang Meng†, Zhongcheng Man*, Quanhui Li*, and Lei Gao*

†,*School of Electrical Engineering, Harbin Institute of Technology, Harbin, China

Abstract

In this paper, two large current rectifiers are proposed based on two wye-connected autotransformers. The requirements of the ideal large current rectifier are analyzed, and it is concluded that the large current rectifier has a higher power density and a higher energy conversion efficiency when it is made up of two three-phase half-wave rectifiers and a wye-connected autotransformer. According to theoretical analysis results, the two novel wye-connected autotransformers are designed to feed two three-phase half-wave rectifiers. The two autotransformers can generate two groups of three-phase voltages with a 60o phase shifting, and their kVA ratings account for 95% and 80% of the load power, respectively. These values are less than those of a double star rectifier at 30% and 46%. From the input mains and output side, the power quality of the proposed rectifiers is the same as that of the double star rectifier. Some experiments validate the correctness of the theoretical analysis.

Key words: Double star rectifier (DSR), Large current rectifier, Three-phase half-wave rectifier, Wye-connected autotransformer

I. INTRODUCTION

Large current rectifiers are used extensively in electrochemical engineering applications, such as plasma-arc generation and micro-arc oxidation [1], [2]. In these applications, the front-end of the power supply is usually a large current rectifier, and the back-end of the power supply is a DC-DC converter which is used to control the output current or output voltage of the power supply [3]. This topology is also called a chopper-rectifier [4]. Since the large current rectifier operates under large current conditions, its conduction losses cannot be ignored. The input mains of the large current rectifier are always connected to a transformer, which significantly affects the power density of the power supply. Therefore, in the chopper-rectifier topology, it is very important to improve the energy conversion efficiency and power density of the front-end rectifier.

Generally, the double star rectifier and the parallel-connected multi-pulse rectifier (MPR) are the two most common topologies for large current rectifiers [5]-[8]. In the MPRs, two or more diode bridge rectifiers are connected in parallel to double the load current, and an isolated transformer or autotransformer is used as the phase-shifting transformer [9]-[15]. In the DSR, a double-star transformer is used as the phase-shifting transformer, and is connected with two three-phase half-wave rectifiers that are also connected in parallel to double the load current [16], [17]. In general, the kVA rating of the phase-shifting transformer determines the power density. The windings of the autotransformer are mutually connected, and the magnetic coupling transmits only part of the load power. However, when the isolated transformer is used as the phase-shifting transformer, all of the load power is transmitted by the magnetic coupling. Therefore, when an equal load power is transmitted, the autotransformer's kVA rating is less than that of the isolated transformer. Furthermore, the power density of the MPR using an autotransformer is greater than that of the DSR and the MPR using an isolated transformer. Under the same load current, for different large current rectifiers, the energy conversion efficiency is determined by the number of rectifying devices, and fewer rectification devices means a higher energy conversion efficiency. In the DSR, six diodes or thyristors are used. In the MPR, at least 12 diodes or thyristors are used. Therefore, the energy conversion efficiency of the DSR is higher than those of the MPRs.

Above all, from the perspective of improving the power density, the autotransformer should be used as the phase-

Manuscript received Apr. 12, 2018; accepted Sep. 14, 2018
Recommended for publication by Associate Editor Yun Zhang.
†Corresponding Author: mfg0327@sina.com
Tel: +86-631-5687068, Harbin Institute of Technology
*School of Electrical Engineering, Harbin Institute of Technology, China

shifting transformer. Meanwhile, from the perspective of improving the energy conversion efficiency, two three-phase half-wave rectifiers should be connected to the output side of the autotransformer. Therefore, an ideal large current rectifier should be made up of an autotransformer and two three-phase half-wave rectifiers. In some applications, such as the power systems of long-range rocket launchers, isolation is not necessary, and the combination of two three-phase half-wave rectifiers and an autotransformer is preferred. In this paper, two low kVA rating wye-connected autotransformers are proposed as a phase-shifting transformer. Unlike the wye-connected autotransformer in [18]-[22], two three-phase half-wave rectifiers, instead of three-phase bridge rectifiers, are connected to the output sides of the two proposed autotransformers. Therefore, when compared with the rectifiers in [18]-[22], the proposed two rectifiers have lower conduction losses under the same load current.

II. Topologies of the Two Proposed Rectifiers

Fig. 1 shows the two proposed rectifier topologies when wye-connected autotransformers are used as the phase-shifting transformer. In Fig. 1(a) and Fig. 1(b), the wye-connected autotransformers operate as step-down and step-up transformers, respectively. Both of the wye-connected autotransformers output two groups of three-phase voltages, which feed two three-phase half-wave rectifiers. The inter-phase reactor (IPR) can absorb the output voltages' instantaneous difference of the two three-phase half-wave rectifiers. In this section, the winding configurations of the two wye-connected autotransformers are analyzed, and the load voltages and input line currents of the two proposed rectifiers are calculated.

A. Requirements of the Phase-Shifting Angle

In a DSR, the double-star transformer can output two groups of three-phase voltages that have a 120° phase difference. Because the output voltage period of the three-phase half-wave rectifier is 120°, the output voltage trough of one of the three-phase half-wave rectifiers corresponds to the output voltage crest of another rectifier, and the load voltage of the DSR contains six pulses per power supply cycle. In fact, when the phase difference between the two groups of three-phase voltages is 60°, the output voltage trough of one three-phase half-wave rectifier corresponds to the output voltage crest of another rectifier [24]. In Fig. 1, the wye-connected autotransformer can output two groups of three-phase voltages which have a 60° phase difference.

B. Winding Configurations of the Proposed Autotransformers

In this part, two wye-connected autotransformers are proposed, both of which can output two groups of three-phase voltages with a 60° phase difference. In Fig. 2(a) and (b), the phasor

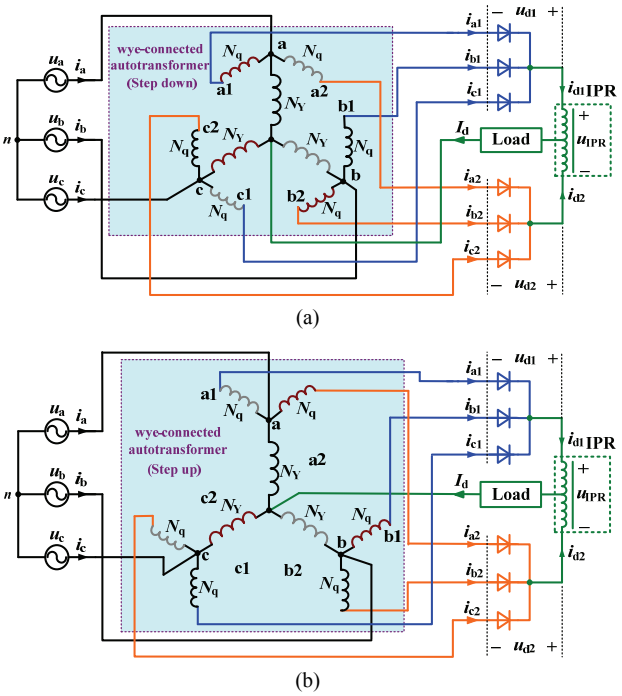

Fig. 1. Proposed rectifier topology: (a) Phase-shifting transformer operating as a step-down transformer; (b) Phase-shifting transformer operating as a step-up transformer.

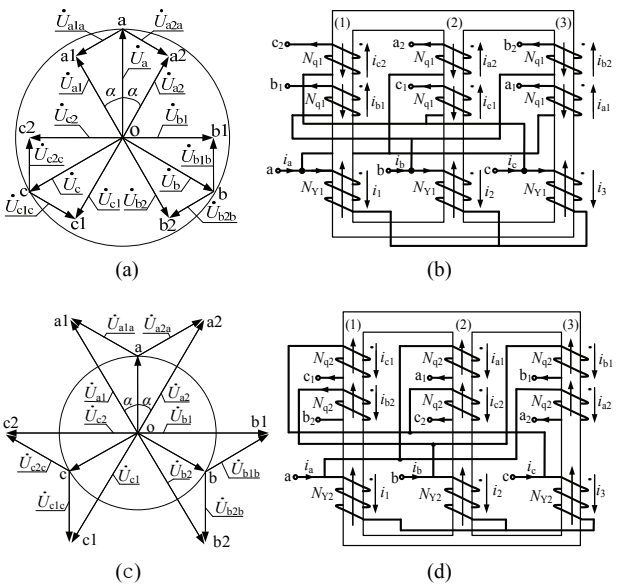

Fig. 2. Phasor diagrams and winding configurations of the proposed autotransformers: (a) Phasor diagram of proposed autotransformer I; (b) Winding configuration of proposed autotransformer I; (c) Phasor diagram of proposed autotransformer II; (d) Winding configuration of proposed autotransformer II.

diagram and winding configuration of proposed autotransformer Ⅰ are illustrated, respectively. In Fig. 2(c) and (d), the phasor diagram and winding configuration of proposed autotransformer Ⅱ are illustrated.

In Fig. 2(a), N_{q1} and N_{Y1} denote the turn numbers of the

extended windings and the wye-connected windings of proposed autotransformer Ⅰ, respectively. In this case, α is equal to 30°. From the winding configuration, the phasor **a1a** is parallel to the phasor **co**, $\angle$**a1ao** is equal to 60°, and the triangle $\angle$**aa1o** is a right triangle. Therefore, the relation between N_{Y1} and N_{q1} meets the following:

$$\frac{N_{q1}}{N_{Y1}}=\frac{1}{2} \tag{1}$$

Similarly, in Fig. 2(c) and Fig. 2(d), the relation between N_{Y2} and N_{q2} meets the following:

$$N_{q2}=N_{Y2} \tag{2}$$

where N_{q2} and N_{Y2} denote the turn numbers of the extended windings and the wye-connected windings of proposed autotransformer Ⅱ, respectively.

The input three-phase phase voltages of the autotransformer are assumed as:

$$\begin{cases} u_a=\sqrt{2}U_m\sin\omega t \\ u_b=\sqrt{2}U_m\sin(\omega t-120^o) \\ u_c=\sqrt{2}U_m\sin(\omega t+120^o) \end{cases} \tag{3}$$

where U_m is the rms value of the input three-phase phase voltages.

From Fig. 2(b), when autotransformer Ⅰ is used:

$$\begin{cases} u_{a1}=\dfrac{\sqrt{6}}{2}U_m\sin(\omega t+30^o) \\ u_{b1}=\dfrac{\sqrt{6}}{2}U_m\sin(\omega t-90^o) \\ u_{c1}=\dfrac{\sqrt{6}}{2}U_m\sin(\omega t+150^o) \end{cases} \quad \begin{cases} u_{a2}=\dfrac{\sqrt{6}}{2}U_m\sin(\omega t-30^o) \\ u_{b2}=\dfrac{\sqrt{6}}{2}U_m\sin(\omega t-150^o) \\ u_{c2}=\dfrac{\sqrt{6}}{2}U_m\sin(\omega t+90^o) \end{cases} \tag{4}$$

From Fig. 2 (d), when autotransformer Ⅱ is used:

$$\begin{cases} u_{a1}=\sqrt{6}U_m\sin(\omega t+30^o) \\ u_{b1}=\sqrt{6}U_m\sin(\omega t-90^o) \\ u_{c1}=\sqrt{6}U_m\sin(\omega t+150^o) \end{cases} \quad \begin{cases} u_{a2}=\sqrt{6}U_m\sin(\omega t-30^o) \\ u_{b2}=\sqrt{6}U_m\sin(\omega t-150^o) \\ u_{c2}=\sqrt{6}U_m\sin(\omega t+90^o) \end{cases} \tag{5}$$

From (4) and (5), the autotransformers in Fig. 2(a) and Fig. 2(c) operate as step-down and step-up transformers, respectively.

C. Analysis of the Input Line Current

When proposed autotransformer Ⅰ is used, the input line current of the rectifier is calculated in this part.

In Fig. 1 and Fig. 2(a), the MMF equations meet the following:

$$\begin{cases} N_{q1}(i_{c2}+i_{b1})-N_{Y1}i_1=N_{q1}(i_{a2}+i_{c1})-N_{Y1}i_2 \\ N_{q1}(i_{a2}+i_{c1})-N_{Y1}i_2=N_{q1}(i_{b2}+i_{a1})-N_{Y1}i_3 \end{cases} \tag{6}$$

where i_{a1}, i_{b1}, i_{c1}, i_{a2}, i_{b2} and i_{c2} are the currents through the extended windings; and i_1, i_2 and i_3 are the currents through the wye-connected windings.

From the Kirchhoff's current law:

$$\begin{cases} i_a=i_1+i_{a1}+i_{a2} \\ i_b=i_2+i_{b1}+i_{b2} \\ i_c=i_3++i_{c1}i_{c2} \\ i_1+i_d+i_3+i_2=0 \end{cases} \tag{7}$$

where i_a, i_b and i_c are the input currents of phase a, b and c. In addition, i_d is the load current.

The input line currents are derived from (1), (6) and (7):

$$\begin{cases} i_a=\dfrac{1}{6}(5i_{a1}+5i_{a2}+2i_{b1}+2i_{c2}-i_{c1}-i_{b2})-\dfrac{1}{3}i_d \\ i_b=\dfrac{1}{6}(5i_{b1}+5i_{b2}+2i_{c1}+2i_{a2}-i_{a1}-i_{c2})-\dfrac{1}{3}i_d \\ i_c=\dfrac{1}{6}(2i_{a1}+5i_{c2}+5i_{c1}+2i_{b2}-i_{a2}-i_{b1})-\dfrac{1}{3}i_d \end{cases} \tag{8}$$

Assume that the two proposed rectifiers operate under a large inductive load, the load current is considered to be constant, and the currents i_{d1} and i_{d2} meet:

$$i_{d1}=i_{d2}=\frac{1}{2}I_d \tag{9}$$

where i_{d1} and i_{d2} are the output currents of the two three-phase half-wave rectifiers, and I_d is the load current.

The input currents of the two three-phase half-wave rectifiers can be expressed as:

$$\begin{cases} i_{a1}=S_{a1}i_{d1} \\ i_{b1}=S_{b1}i_{d1} \\ i_{c1}=S_{c1}i_{d1} \end{cases} \quad \begin{cases} i_{a2}=S_{a2}i_{d2} \\ i_{b2}=S_{b2}i_{d2} \\ i_{c2}=S_{c2}i_{d2} \end{cases} \tag{10}$$

where S_{a1}, S_{b1}, S_{c1}, S_{a2}, S_{b2} and S_{c2} are switch functions of phases a1, b1, c1, a2, b2 and c2, respectively.

Substituting (9) and (10) into (8) yields:

$$\begin{cases} i_a=\dfrac{1}{12}I_d(2S_{b1}+2S_{c2}+5S_{a1}+5S_{a2}-S_{c1}-S_{b2}-4) \\ i_b=\dfrac{1}{12}I_d(2S_{c1}+2S_{a2}+5S_{b1}+5S_{b2}-S_{a1}-S_{c2}-4) \\ i_c=\dfrac{1}{12}I_d(2S_{a1}+2S_{b2}+5S_{c1}+5S_{c2}-S_{b1}-S_{a2}-4) \end{cases} \tag{11}$$

Fig. 3(a) and (b) illustrate the current i_a and its spectrum, respectively. The input line current of the proposed rectifier contains six steps per power supply cycle, which is similar to that of the double-star rectifier and the three-phase bridge rectifier. Similarly, when proposed autotransformer Ⅱ is used, the input line current can also be calculated. Fig. 3(c) and (d) show the input line current and its spectrum, respectively.

D. Analysis of the Load Voltage

From modulation theory, u_{d1} and u_{d2} can be calculated as:

$$\begin{cases} u_{d1}=u_{a1}S_{a1}+u_{b1}S_{b1}+u_{c1}S_{c1} \\ u_{d2}=u_{a2}S_{a2}+u_{b2}S_{b2}+u_{c2}S_{c2} \end{cases} \tag{12}$$

where u_{d1} and u_{d2} are the output voltages of the two three-phase half-wave rectifiers, as shown in Fig. 1.

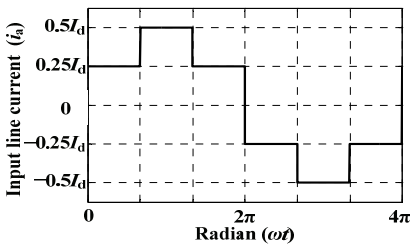

(a)

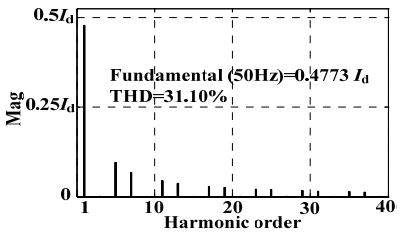

(b)

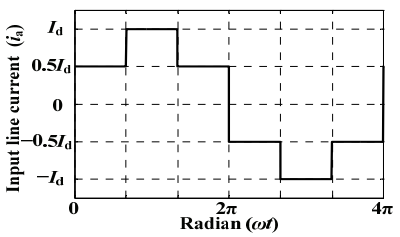

(c)

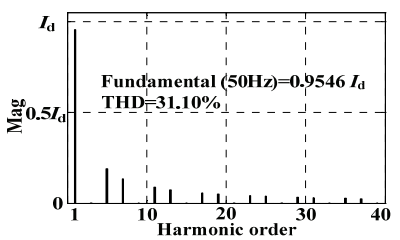

(d)

Fig. 3. Theoretical input currents and their spectrums: (a) Input current when proposed autotransformer I is used; (b) Spectrum of the input current when autotransformer I is used; (c) Input current when proposed autotransformer II is used; (d) Spectrum of the input current when autotransformer II is used.

Substituting (4) into (12) yields:

$$u_{d1}=\begin{cases}\dfrac{\sqrt{6}}{2}U_m\sin(\omega t+30^o-k120^o)\\ \quad \omega t\in[k120^o,k120^o+120^o]\end{cases}$$

$$u_{d2}=\begin{cases}\dfrac{\sqrt{6}}{2}U_m\sin(\omega t+90^o-k120^o)\\ \quad \omega t\in[k120^o,k120^o+60^o]\\ \dfrac{\sqrt{6}}{2}U_m\sin(\omega t-30^o-k120^o)\\ \quad \omega t\in[k120^o+60^o,k120^o+120^o].\end{cases}\quad (13)$$

where k =0,1,2….

Load voltage is equal to the average value of u_{d1} and u_{d2}:

$$u_d=\frac{1}{2}(u_{d1}+u_{d2}) \quad (14)$$

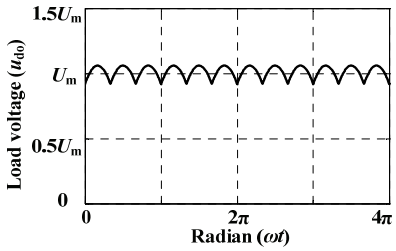

(a)

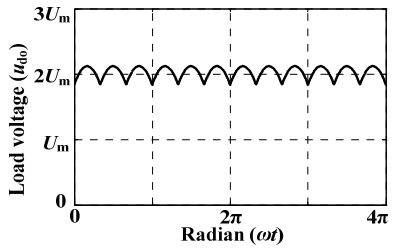

(b)

Fig. 4. Load voltage: (a) When proposed autotransformer I is used; (b) When proposed autotransformer Ⅱ is used.

where u_d is the load voltage.

Substituting (11) into (12) yields:

$$u_{do}=\frac{3\sqrt{2}}{4}U_m\sin(\omega t+60^o-k60^o)\omega t\in[k60^o,(k+1)60^o] \quad (15)$$

Fig. 4(a) shows the load voltage u_{do}. From Fig. 4(a), the load voltage contains six pulses per power supply cycle, which is similar to the three-phase bridge rectifier and the DSR.

Similarly, when proposed autotransformer Ⅱ is used, the load voltage can be calculated and illustrated, as shown in Fig. 4(b).

E. Analysis of the KVA Ratings of the Proposed Autotransformers

In the two proposed rectifiers, a wye-connected autotransformer is the main magnetic devices and it determines the system's power density. In this part, proposed autotransformer Ⅰ is used as an example, and the kVA ratings are calculated.

In order to calculate the kVA rating, it is necessary to calculate the RMS values of the currents through and the voltages across the windings.

From (1) and Fig. 2(b), the rms values of the voltages across the wye-connected windings are equal to U_m, and the rms values of the voltages across the extended-connected windings are equal to $U_m/2$.

From (10), the RMS values of the currents through the extended windings can be calculated as:

$$I_{a1}=I_{b1}=I_{c1}=I_{a2}=I_{b2}=I_{c2}=\frac{\sqrt{3}}{6}I_d \quad (16)$$

where I_{a1}, I_{b1}, I_{c1}, I_{a2}, I_{b2} and I_{c2} are the rms values of the currents through the extended windings.

The currents through the wye-connected windings can derived from (6) and (9):

$$\begin{cases} i_1 = \frac{1}{6}(2i_{c2} + 2i_{b1} - i_{a2} - i_{c1} - i_{b2} - i_{a1}) - \frac{1}{3}i_d \\ i_2 = \frac{1}{6}(2i_{a2} + 2i_{c1} - i_{b1} - i_{a1} - i_{c2} - i_{b2}) - \frac{1}{3}i_d \\ i_3 = \frac{1}{6}(2i_{a2} + 2i_{c1} - i_{b1} - i_{a1} - i_{c2} - i_{b2}) - \frac{1}{3}i_d \end{cases} \quad (17)$$

where I_1, I_2 and I_3 are the rms values of the currents through the wye-connected windings.

Substituting (10) into (17) yields:

$$I_1 = I_2 = I_3 = \frac{\sqrt{2}}{4} I_d \quad (18)$$

Define the kVA rating of the transformer as:

$$S_{kVA,auto} = \frac{1}{2}\sum_{i=1}^{n} U_i I_i \quad (19)$$

where I_i and U_i are the rms values of the current through and the voltage across the winding, respectively.

Therefore, the kVA rating of proposed autotransformer Ⅰ is calculated as:

$$S_{kVA,auto\ I} = \frac{\sqrt{6}(\sqrt{3}+\sqrt{2})}{8} U_m I_d \quad (20)$$

The average value of the load voltage can be derived from (13):

$$U_{do} = \frac{9\sqrt{2}}{4\pi} U_m \quad (21)$$

From (20) and (21), $S_{kVA,auto\ I}$ can be presented as:

$$S_{kVA,auto\ I} = \frac{\pi}{6}(1+\frac{\sqrt{6}}{3}) I_d U_{do} \quad (22)$$

Define the load power as:

$$P_o = U_{do} I_d \quad (23)$$

Substituting (21) into (20) yields:

$$S_{kVA,auto\ I} = 0.9511 P_o \quad (24)$$

From (24), the kVA rating of proposed autotransformer Ⅰ accounts for approximately 95% of the load power.

Similarly, the kVA rating of proposed autotransformer Ⅱ can be calculated, and it accounts for 80% of the load power.

III. Discussion of Rectifiers Using the Proposed Autotransformers

In this section, the proposed rectifiers are compared with the DSR from the viewpoint of energy conversion efficiency, the kVA rating of the phase-shifting transformer, and the power quality. In addition, the proposed rectifiers are also compared with the three-phase diode-bridge rectifier (full-wave rectifier) from the viewpoint of the energy conversion efficiency and power quality. Finally, the proposed rectifiers are compared with the 12-pulse rectifier using the wye-connected autotransformer.

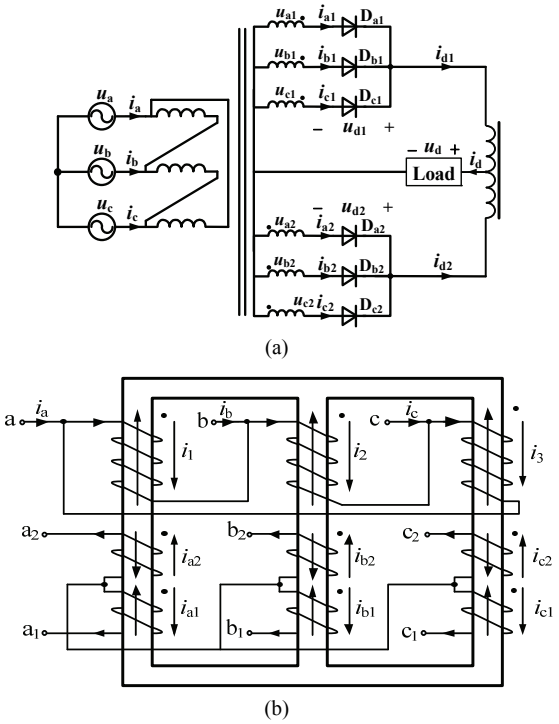

Fig. 5. DSR and winding configuration of a double-star transformer: (a) Topology of the DSR; (b) Winding configuration of the double-star transformer.

A. Comparison of the Proposed Rectifiers with the DSR

- Both of the two proposed rectifiers and the DSR use phase-shifting transformers. In the previously mentioned analysis, the kVA ratings of the two proposed autotransformers account for about 95% and 80% of the load power, respectively. Fig. 5(a) shows the topology of the DSR, and Fig. 5(b) shows the winding configuration of the double-star transformer. As discussed in [24] and [25], the kVA rating of the double-star transformer is about 126% of the load power. Therefore, the kVA ratings of autotransformers Ⅰ and Ⅱ are less than that of a double-star transformer 30% and 46% under the same load power. This means that the two proposed rectifiers have higher power densities than the DSR.
- When the two proposed autotransformers are applied to rectifiers, both of the output terminals of the autotransformers connect with two three-phase half-wave rectifiers. In both of the two proposed rectifiers, the number of rectifying devices is equal to that of the DSR. Therefore, the energy conversion efficiencies of the proposed rectifiers are approximately equal to that of the DSR under the same load current.
- When the two proposed autotransformers are applied to large current rectifiers, the input line current contains

six steps per power supply cycle, and the load voltage contains six pulses per power supply cycle, both of which are the same as those of the DSR. Therefore, from the input mains and the output side, the two proposed rectifiers have the same power quality as the DSR.

B. Comparison of the Proposed Rectifiers with the Three Phase Full-Wave Rectifier

Energy conversion efficiency is related to the conduction losses for the proposed rectifiers and the three-phase full-wave rectifier. The conduction loss per power supply cycle can be presented as:

$$P_{\mathrm{CL}} = NI_{\mathrm{t}}U_{\mathrm{t}}t_{\mathrm{C}} \tag{25}$$

where N is the number of rectification devices. In the two proposed rectifiers and the three-phase full-wave rectifier, N=6. I_{t} is the on-state current of the rectification device for the two proposed rectifiers, and it is equal to $I_{\mathrm{d}}/2$. Meanwhile, for the three-phase full-wave rectifier, I_{t} is equal to I_{d}. U_{t} is the forward voltage drop, t_{C} is the conduction time per power supply cycle, and t_{C} is equal to 0.02/3s.

From (25), the conduction loss per power supply cycle of the two proposed rectifiers is calculated as:

$$P_{\mathrm{CL,P}} = 6\frac{I_{\mathrm{d}}}{2}U_{\mathrm{t}}\frac{0.02}{3} = 0.02I_{\mathrm{d}}U_{\mathrm{t}} \tag{26}$$

In the three-phase full-wave rectifier, the conduction loss per power supply cycle is calculated as:

$$P_{\mathrm{CL,T}} = 6I_{\mathrm{d}}U_{\mathrm{t}}\frac{0.02}{3} = 0.04I_{\mathrm{d}}U_{\mathrm{t}} \tag{27}$$

From (26) and (27), under the same load current, the conduction losses of the two proposed rectifiers are half that of the three-phase full-wave rectifier.

C. Comparison of the Proposed Rectifiers with the 12-Pulse Rectifier Using the Wye-Connected Autotransformer

1) The Phase-shifting Angle of the Wye-connected Autotransformer:

Although the wye-connected autotransformer has already been used in MPR, it has never fed two three-phase half-wave rectifiers. In [7], [18], two wye-connected autotransformers were designed and applied to 12-pulse and 18-pulse rectifiers, respectively. Therefore, the rectifiers proposed in [7] and [18] are combinations of two or three three-phase diode bridge rectifiers and a wye-connected autotransformer. As discussed in [15], when an autotransformer feeds two three-phase diode-bridge rectifiers, its phase-shifting angle is 15°. Meanwhile, when an autotransformer feeds two three-phase half-wave rectifiers, its phase-shifting angle is 30°. Therefore, if autotransformers feed different types of rectifiers, their phase-shifting angles are also different.

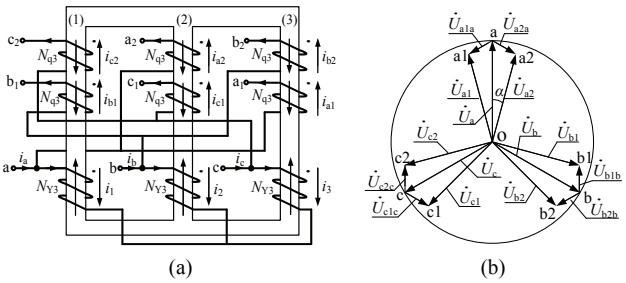

Fig. 6. Winding configuration and phasor diagram of the wye-connected autotransformer in a 12-pulse rectifier: (a) Winding configuration; (b) Phasor diagram.

2) Winding Configuration of the Wye-connected Autotransformer:

When the phase-shifting angles of the autotransformers are different, the winding configurations of the autotransformer are inevitably different. Fig. 6 shows the winding configuration and its phasor diagram when the wye-connected autotransformer is used in a 12-pulse rectifier. In Fig. 6(b), α is equal to 15°. From Fig. 2(a) and Fig. 6(a), when α is equal to 15°, the winding configuration of the wye-connected autotransformer is similar with that when α is equal to 30°.

In Fig. 2(a), the ratio of N_{Y1} to N_{q1} is equal to 0.5. From Fig. 6, the ratio of N_{Y3} to N_{q3} meets:

$$\frac{N_{\mathrm{q3}}}{N_{\mathrm{Y3}}} = 2-\sqrt{3} \tag{28}$$

Although the winding configurations of the wye-connected autotransformers in Fig. 4(a) and Fig. 6(a) are similar, their turn ratios are different. Therefore, the two proposed autotransformers are different from those in [7] and [19].

3) Actual Functioning of the Wye-connected Autotransformer:

The actual functioning of the wye-connected autotransformer is different under different phase-shifting angles. This part compares the actual functioning of autotransformer Ⅰ and the autotransformer in Fig. 6(a).

From (10) and (17), in proposed autotransformer Ⅰ, the currents through the windings can be derived, as shown in Fig. 7(a). Similarly, from MMF equations and Kirchhoff's current law, the currents through the windings in Fig. 6(a) can be derived, as shown in Fig. 7(b). From Fig. 7, when the wye-connected autotransformer feeds two three-phase half-wave rectifiers, the currents through its windings are unidirectional, which is entirely different from when it feeds two three-phase diode-bridge rectifiers.

4) Conduction Losses

From Fig. 6, for a 12-pulse rectifier, 12 diodes are used and the current through the 12 diodes is equal to I_{d} when they turn on. From (36), the conduction loss per power supply cycle of the 12-pulse rectifiers is calculated as:

$$P_{\mathrm{CL,12}} = 12I_{\mathrm{d}}U_{\mathrm{t}}\frac{0.02}{3} = 0.08I_{\mathrm{d}}U_{\mathrm{t}} \tag{29}$$

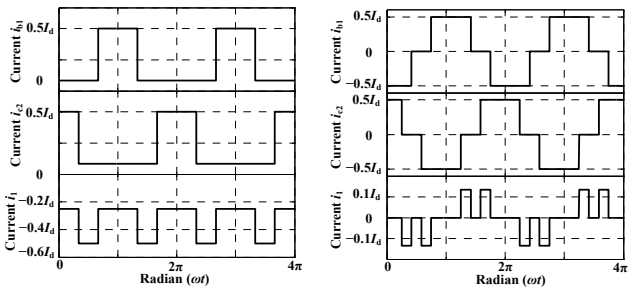

(a) (b)

Fig. 7. Currents through the windings of the wye-connected autotransformer: (a) Phase-shifting angle is 15°; (b) Phase-shifting angle is 30°.

TABLE I
COMPARISON OF THE TWO PROPOSED RECTIFIERS AND THE 12-PULSE RECTIFIER USING THE WYE-CONNECTED AUTOTRANSFORMER

	The two proposed rectifiers	12-pulse rectifier
Number of the rectification devices	6	12
Phase-shifting angle of the autotransformer	15°	30°
Conduction losses of the rectification devices	$0.02I_dU_t$	$0.08I_dU_t$
Pulse number of the load voltage	6	12
Step number of the input current	6	12
If the ZSBT is needed?	No	Yes

From (29), under the same load current, it is observed that the conduction loss per power supply cycle of the two proposed rectifiers is a quarter of that of the12-pulse rectifier.

Table I summarizes a comparison of the two proposed rectifiers and the 12-pulse rectifier using the wye-connected autotransformer.

From Table I, the conduction losses of the two proposed rectifiers are far less than that of the 12-pulse rectifier, which is very important under a large load current. In the two proposed rectifiers, both the pulse number of the load voltage and the step number of the input current are six, which are less than those of the 12-pulse rectifier. Theoretically, under a large inductive load, the THD of the input line current in the two proposed rectifiers is 31%, and the THD of the input line current in the 12-pulse rectifier is 15.2%. Therefore, from the viewpoint of power quality, the 12-pulse rectifier is better than the two proposed rectifiers. However, the power quality of the two proposed rectifiers and that of the 12-pulse rectifier fail to meet IEEE Standard 519-1992. As a result, harmonic reduction installations are needed in applications. In the two proposed rectifiers, ZSBT is not needed. However, in the 12-pulse rectifier using the wye-connected autotransformer, ZSBT is necessary.

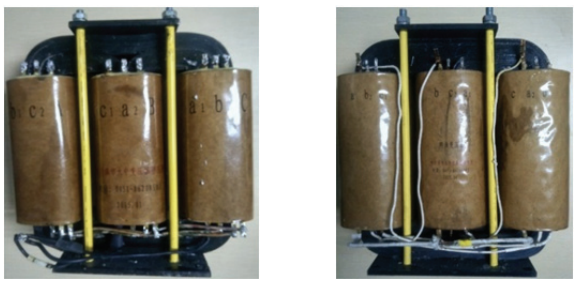

(a) (b)

Fig. 8. Pictures of the two autotransformers: (a) Proposed autotransformer Ⅰ; (b) Proposed autotransformer Ⅱ.

TABLE II
PARAMETERS OF AUTOTRANSFORMER I

Parameter	Value
Turn numbers of the wye-connected winding	176
Turn numbers of the extended winding	88
Wire diameter of the wye-connected winding	2.0mm
Wire diameter of the extended winding	1.88mm
Core lamination	50 mm
Core width	80 mm
Wire packet height	100 mm
Rated apparent power	3500 VA
Load power to be transmitted	3680 W

IV. EXPERIMENTAL RESULTS

In order to validate the above theoretical analysis, two wye-connected autotransformers with 60° phase-shifting angles are manufactured and applied to rectifiers. Then a number of experiments are carried out. In order to verify the universality of the methods, the experimental conditions for the two rectifiers are different. When experimenting on proposed autotransformer Ⅰ, the load resistance is 15Ω and the rms value of the input voltage is equal to 230V. Meanwhile, when experimenting on proposed autotransformer Ⅱ, the load resistance is 22.5Ω and the rms value of the input voltage is equal to 220V.

A. Parameters of the Two Proposed Autotransformers

Fig. 8 shows the two autotransformers. An air gap is not required in the two proposed autotransformers. Table II and Table III show the parameters of proposed autotransformers Ⅰ and Ⅱ, respectively.

B. Phase-Shift Performance of the Two Proposed Autotransformers

Fig. 9(a) and (b) show the input and output voltages of the two proposed autotransformers. In Fig. 9, the phase differences between u_{a1} and u_{a2}, between u_{a1} and u_a, and between u_{a2} and u_a, are about 60°, 30° and 30°, respectively. These results are coincident with the theoretical analysis.

Fig. 9(c) and (d) show the voltages across the windings. In

TABLE III
PARAMETERS OF AUTOTRANSFORMER II

Parameter	Value
Turn numbers of the wye-connected winding	176
Turn numbers of the extended winding	176
Wire diameter of the wye-connected winding	2×3.5mm
Wire diameter of the extended winding	2.12mm
Core lamination	50 mm
Core width	80 mm
Wire packet height	220 mm
Rated apparent power	6800 VA
Load power to be transmitted	8500 W

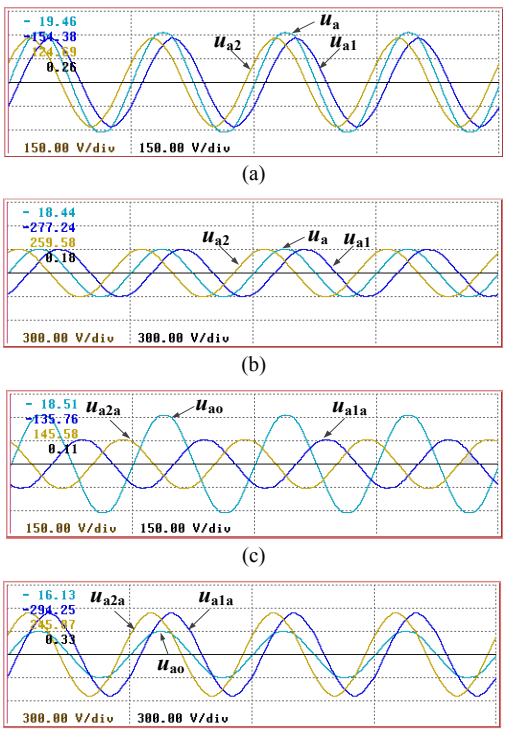

Fig. 9. Input voltage, output voltages, and voltages across the windings of the two proposed autotransformers: (a) Input and output voltages of proposed autotransformer Ⅰ; (b) Input and output voltages of proposed autotransformer Ⅱ; (c) Voltages across windings **ao**, **a1a** and **a2a** of autotransformer Ⅰ; (d) Voltages across windings **ao**, **a1a** and **a2a** of autotransformer Ⅱ.

Fig. 9(c) and (d), the phase differences between u_{a1a} and u_{a2a}, between u_{a1a} and u_{ao}, and between u_{a2a} and u_{ao}, are all 120°. These results are also coincident with the theoretical analysis in Fig. 2(b) and Fig. 2(d).

From Fig. 9, it can be seen that both of the proposed autotransformers can realize the required phase-shifting angle.

C. Input Line Current of the Proposed Rectifiers

When proposed autotransformer Ⅰ is used, Fig. 10(a) shows the input line currents, and their rms values are 5.185A, 5.187A and 5.184A, respectively. The THD values of the input line currents are 29.21%, 28.53% and 29.27%, respectively. When proposed autotransformer Ⅱ is used, Fig. 10(b) shows the input line currents. The rms values are 13.830A, 13.970A and 14.215A, respectively. In addition, their THD values are 27.00%, 28.52% and 28.11%, respectively. From Fig. 10, the input currents contain six steps per power supply cycle, which is coincident with the theoretical analysis.

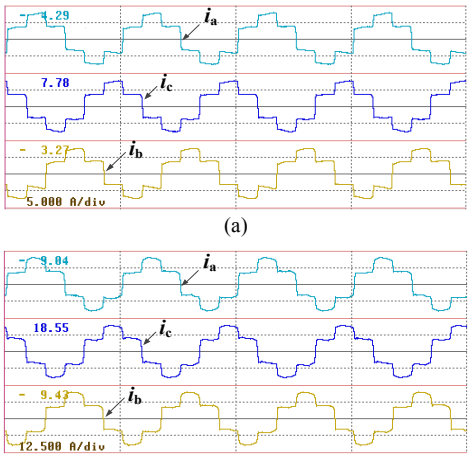

Fig. 10. Input currents: (a) When proposed autotransformer Ⅰ is used; (b) When proposed autotransformer Ⅱ is used.

D. KVA Rating of Proposed Autotransformer Ⅰ

Fig. 11(a) shows the current through and the voltage across the wye-connected winding of proposed autotransformer Ⅰ. Proposed autotransformer Ⅰ is assumed to be symmetrical, and from Fig. 11(a), the apparent power of the wye-connected windings is calculated as:

$$S_{\text{kVA,ST I}} = \frac{1}{2} \times 3 \times 231 \times 5.38 = 1864.2\text{VA} \tag{30}$$

Fig. 11. Voltage across and current through the windings of the two proposed autotransformers, along with the load voltage and load current: (a) Voltage across and current through the wye-connected winding of proposed autotransformer I; (b) Voltage across and current through the extended winding of proposed autotransformer I; (c) Load voltage and load current when proposed autotransformer I is used; (d) Current through and voltage across the wye-connected winding of proposed autotransformer II; (e) Voltage across and current through the extended winding of autotransformer II; (f) Load current and load voltage when proposed autotransformer II is used.

Fig. 11(b) shows the current through and voltage across the extended winding of proposed autotransformer Ⅰ. The apparent power of the extended windings can be calculated as:

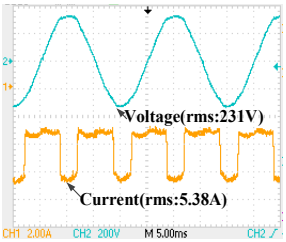

(a) Voltage across and current through the wye-connected winding of proposed autotransformer Ⅰ.

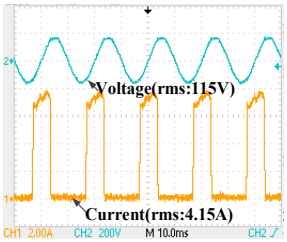

(b) Voltage across and current through the extended winding of proposed autotransformer Ⅰ.

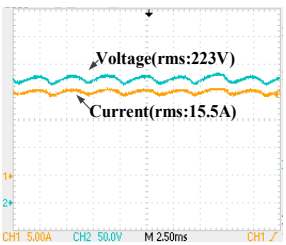

(c) Load voltage and load current when proposed autotransformer Ⅰ is used.

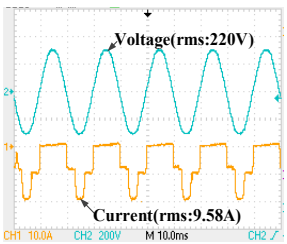

(d) Current through and voltage across the wye-connected winding of proposed autotransformer Ⅱ.

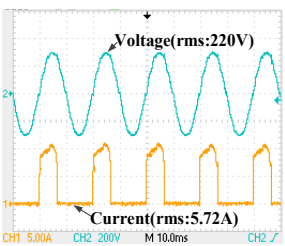

(e) Voltage across and current through the extended winding of autotransformer Ⅱ.

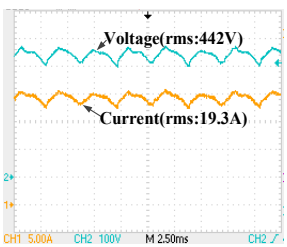

(f) Load current and load voltage when proposed autotransformer Ⅱ is used.

Fig. 11. Voltage across and current through the windings of the two proposed autotransformers, along with the load voltage and load current: (a) Voltage across and current through the wye-connected winding of proposed autotransformer I; (b) Voltage across and current through the extended winding of proposed autotransformer I; (c) Load voltage and load current when proposed autotransformer I is used; (d) Current through and voltage across the wye-connected winding of proposed autotransformer II; (e) Voltage across and current through the extended winding of autotransformer II; (f) Load current and load voltage when proposed autotransformer II is used.

$$S_{\text{kVA,EX I}} = 0.5 \times 6 \times 115 \times 4.15 = 1431.8\text{VA} \tag{31}$$

From (30) and (31), the apparent power of proposed autotransformer Ⅰ is 3296VA.

Fig. 11(c) shows the load current and load voltage when proposed autotransformer Ⅰ is used. Both the load current and load voltage contain six pulses per power supply cycle under a resistive load. From Fig. 11(c), the load power is calculated as 3456.5W.

The ratio of the autotransformer's apparent power to the load power is:

$$S_{\text{auto I}} = \frac{3296}{3456.5} \times 100\% \approx 95.4\% \tag{32}$$

Therefore, when experimenting, the proposed autotransformer's kVA rating is 95.4% of the load power, which is identified with the theoretical value.

E. KVA Rating of Autotransformer II

Fig. 11(d) shows the current through and voltage across the wye-connected winding of proposed autotransformer Ⅱ. Fig. 11(e) shows the current through and voltage across the extended winding. Fig. 11(f) shows the load current and load voltage.

From Fig. 11(d) and (e), the apparent power of the wye-connected windings is calculated as:

$$S_{\text{kVA,ST II}} = 0.5 \times 3 \times 220 \times 9.58 = 3161.4\text{VA} \tag{33}$$

and the apparent power of the extended windings is calculated as:

$$S_{\text{kVA,EX II}} = 0.5 \times 6 \times 220 \times 5.72 = 3775.2\text{VA} \tag{34}$$

From (33) and (34), the autotransformer's apparent power is 6936.6VA.

From Fig. 11(f), the load power is 8530.6W. Therefore, the ratio of the apparent power of proposed autotransformer Ⅱ to the load power is:

$$S_{\text{auto II}} = \frac{6936.6}{8530.6} \times 100\% \approx 81.3\% \tag{35}$$

From (35), when experimenting, the kVA rating is approximately 81% of the load power, which is also identified with the theoretical value.

V. Conclusion

In this paper, two wye-connected autotransformers are proposed and used in two large current rectifiers. The following conclusions are obtained:

- The novel large current rectifier is a combination of a wye-connected autotransformer and two three-phase half-wave rectifiers. Although the wye-connected autotransformer has already been used in MPR, it is used to feed the three-phase diode-bridge rectifiers in MPR. It has never been used to feed three-phase half-wave rectifiers. When the autotransformer is used to feed three-phase half-wave rectifiers, its phase-shifting angle is different from that when it feeds three-phase bridge rectifiers. The different phase-shifting angles inevitably lead to different winding configurations. In addition, when a wye-connected autotransformer and two three-phase half-wave rectifiers are combined to form a large current rectifier, the conduction losses of the rectifying devices are less than those of the MPR under the same load current.
- The kVA ratings of autotransformers Ⅰ and Ⅱ are

less than that of the double-star transformer 30% and 46% under the same load power. Therefore, the power density of the two proposed rectifiers are higher than that of the DSR.

- The conduction losses of the two proposed rectifiers are lower than that of the MPR, and are equal to that of the DSR under the same load current.
- From both the input mains and the output side, the power qualities of the two proposed rectifiers are the same as that of the DSR.
- In the proposed rectifiers, the theoretical THD value of the input current is 31%, and the experimental THD value is about 29%. Both of these values are larger than those of the MPR. In future research, some filters will be installed to reduce the harmonics.

Above all, the energy conversion efficiency of the two proposed rectifiers is higher than that of the MPR. In addition, it is equal to that of the DSR under the same load current. The two proposed rectifiers have higher power densities than the DSR under the same load current. Therefore, when isolation is not necessary, the two proposed rectifiers are the best choice under a large load current.

REFERENCES

[1] J. R. Rodriguez, J. Pontt, C. Silva, E. P. Wiechmann, P. W. Hammond, F. W. Santucci, R. Alvarez, S. Kouro, and P. Lezana, "Large current rectifiers: State of the art and future trends," *IEEE Trans. Ind. Electron.*, Vol. 52, No. 3, pp. 738-746, Jun. 2005.

[2] F. Carastro, A. Castellazzi, J. Clare, and P. Wheeler, "High-efficiency high-reliability pulsed power converters for industrial processes," *IEEE Trans. Power Electron.*, Vol.27, No.1, pp.37-45, Jan. 2012

[3] W. Yang, S. Yang, and H. Liu, "Micro-arc oxidation flyback switching current pulse unit and combination of multi-units," *2012 IEEE 7th International Power Electronics and Motion Control Conference - ECCE Asia*, 2012, pp. 2952-2956.

[4] J. Solanki, N. Fröhleke, J. Böcker, and A. Averberg, "High-current variable-voltage rectifiers: State of the art topologies," *IET Power Electronics*, Vol. 8, No. 6, pp. 1068-1080, 2015.

[5] B. Singh, S. Gairola, B. N. Singh, A. Chandra, and K. Alhadded, "Multi-pulse AC-DC converters for improving power quality: a review," *IEEE Trans. Power Electron.*, Vol. 23, No. 1, pp. 260-281, Jan. 2008.

[6] P. Aqueveque, E. P. Wiechmann, and R. P. Burgos, "On the efficiency and reliability of high-current rectifiers," *IEEE Power Electronics Specialists Conference*, pp. 4509-4516, 2008.

[7] R. C. Fernandes, P. S. Oliveira, and F. J. M. Seixas, "A family of autoconnected transformers for 12- and 18-pulse converters-generalization for delta and wye topologies," *IEEE Trans. Power Electron.*, Vol. 26, No. 7, pp. 2065-2078, Apr. 2011.

[8] C. Young, M. Chen, C. Lai, and D. Shih, "A novel active interphase transformer scheme to achieve three-phase line current balance for 24-pulse converter," *IEEE Trans. Power Electron.*, Vol. 27, No. 4, pp. 1719-1731, Apr. 2012.

[9] F. Meng, W. Yang, and S. Yang, "Effect of voltage transformation ratio on the kilovoltampere rating of delta-connected autotransformer for 12-pulse rectifier system," *IEEE Trans. Ind. Electron.*, Vol. 60, No. 9, pp. 3579-3588, Sep. 2013.

[10] R. Kalpana, G. Bhuvaneswari, and B. Singh, "Autoconnected transformer based 20-pulse AC-DC converter for telecommunication power supply," *IEEE Trans. Ind. Electron.*, Vol. 60, No. 10, pp. 4178-4190, Oct. 2013.

[11] F. Meng, L. Gao, S. Yang, and W. Yang, "Effect of single-phasing on multipulse rectifier with active interphase reactor," *IEEE Trans. Power Electron.*, Vol. 30, No. 5, pp.2549-2555, Jan. 2015.

[12] A. Gerlando, G. M. Foglia, M. F. Iacchetti, and M. Ubaldini, "Optimized coil arrangement in wound interphase reactors for high-power rectifier systems," *IEEE Trans. Energy Convers.*, Vol. 29, No. 3, pp. 652-662, Sep. 2014.

[13] J. Sandoval, H. Krishnamoorthy, P. Enjeti, "Reduced active switch front end multi-pulse rectifier with medium frequency transformer isolation," *IEEE Trans. Power Electron.*, Vol. 32, No. 10, pp. 7458-7468, Oct. 2017.

[14] J. Solanki, N. Fröhleke, and J. Böcker, "Implementation of hybrid filter for 12-pulse thyristor rectifier supplying high-current variable-voltage dc load," *IEEE Trans. Ind. Electron.*, Vol. 62, No. 8, pp. 4691-4701, Aug. 2015.

[15] D. A. Paice, Power Electronic Converter Harmonic Multipulse Methods for Clean Power, New York: IEEE Press, 1996.

[16] J. Wang, S. Yang, and W. Yang, "A low harmonic double wye rectifier with current injection at DC side," *International Electronics and Application Conference and Exposition*, pp. 909-913, 2014.

[17] J. A. Garcia and G. Moon, "A high-efficiency three-phase zvs pwm converter utilizing a positive double-wye active rectifier stage for server power supply," *IEEE Trans. Ind. Electron.*, Vol.58, No.8, pp. 3317-3329, Aug. 2011.

[18] J. Ferens, H. D. Hajdinjak, and S. Rhodes, "18-pulse rectification system using a wye-connected autotransformer," U.S. Patent 6650557 B2, Nov. 18, 2003.

[19] B. Singh and S. Gairola, "A fork connected auto-transformer based 24-pulse AC-DC converter," *India International Conference on Power Electronics 2006*, pp. 1391-1396, 2006.

[20] R. Abdollahi and A. Jalilian, "Fork-connected autotransformer based 30-pulse ac-dc converter for power quality improvement," *Int. J. Electr. Eng. Informat.*, Vol. 4, No. 2, 2012.

[21] R. Abdollahi, "Delta/fork-connected transformer-based 36-pulse ac-dc converter for power quality improvement," *J. Electr. Contr. Eng.*, Vol. 2, No. 2, 2012.

[22] B. Liu, S. Duan, and C. Qiu, "Research on 18-pulse rectifier based on a Boost star-fork connected autotransformer," 2011 *International Conference on Electrical Machine and Systems*, pp. 1-4, 2011.

[23] F. Meng, X. Xu, L. Gao, and C. Cai, "Active harmonic reduction using DC-side current injection applied in a novel large current rectifier based on fork-connected autotransformer," *IEEE Trans. Ind. Electron.*, Vol. 64, No. 7, pp. 5250-5264, Jul. 2017.

[24] F. Meng, P. Liu, and L. Gao, "Optimal design of star-connected autotransformer applied to large current rectifier," *IET Electric Power Appl.*, Vol. 11, No. 1, pp. 80-89, Jan. 2017.

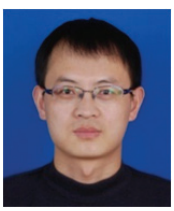

Fangang Meng was born in Shandong, China, in 1982. He received his B.S. degree in Thermal Energy and Power Engineering, and his M.S. and Ph.D. degrees in Electrical Engineering from the Harbin Institute of Technology, Harbin, China, in 2005, 2007 and 2011, respectively. Since 2011, he has been working as an Assistant Professor at the Harbin Institute of Technology, Weihai, China. His current research interests include harmonics detection, stability analysis of converters and high power rectification.

Zhongcheng Man was born in Shandong, China, in 1993. He received his B.S. degree in Electrical Engineering from the China University of Mining and Technology, Xuzhou, China, in 2017. Since 2017, he has been working towards his M.S. degree in Power Electronics and Power Drives at the Harbin Institute of Technology, Weihai, China. His current research interests include multi-pulse rectifiers, power electronic transformers and high-power rectification.

Quanhui Li was born in Shandong, China, in 1996. He received his B.S. degree in Electrical Engineering from the Harbin Institute of Technology, Weihai, China, in 2018, where he is presently working towards his M.S. degree in Power Electronics and Power Drives. His current research interests include multi-pulse rectifiers and high-power rectification.

Lei Gao was born in Hebei, China, in 1982. She received her B.S., M.S. and Ph.D. degrees in Electrical Engineering from the Harbin Institute of Technology, Harbin, China, in 2005, 2007 and 2012, respectively. Since 2012, she has been working as an Assistant Professor at the Harbin Institute of Technology, Weihai, China. Her current research interests include power electronics and motor drives.